Current Biology 21, 1118–1122, July 12, 2011 ©2011 Elsevier Ltd All rights reserved DOI 10.1016/j.cub.2011.05.022

Report

From Part- to Whole-Body Ownership in the Multisensory Brain

Valeria I. Petkova,[1,*] Malin Björnsdotter,[1,3] Giovanni Gentile,[1,3] Tomas Jonsson,[2] Tie-Qiang Li,[2] and H. Henrik Ehrsson[1]

[1]Brain, Body & Self Laboratory, Department of Neuroscience, Karolinska Institutet, Retzius väg 8, SE-171 77 Stockholm, Sweden

[2]Department of Medical Physics, Karolinska University Hospital Huddinge, SE-141 86 Stockholm, Sweden

Summary

The question of how we experience ownership of an entire body distinct from the external world is a fundamental problem in psychology and neuroscience [1–6]. Earlier studies suggest that integration of visual, tactile, and proprioceptive information in multisensory areas [7–11] mediates self-attribution of single limbs. However, it is still unknown how ownership of individual body parts translates into the unitary experience of owning a whole body. Here, we used a "body-swap" illusion [12], in which people experienced an artificial body to be their own, in combination with functional magnetic resonance imaging to reveal a coupling between the experience of full-body ownership and neural responses in bilateral ventral premotor and left intraparietal cortices, and left putamen. Importantly, activity in the ventral premotor cortex reflected the construction of ownership of a whole body from the parts, because it was stronger when the stimulated body part was attached to a body, was present irrespective of whether the illusion was triggered by stimulation of the hand or the abdomen, and displayed multivoxel patterns carrying information about full-body ownership. These findings suggest that the unitary experience of owning an entire body is produced by neuronal populations that integrate multisensory information across body segments.

Results and Discussion

When we look down at our body, we immediately experience that it belongs to us. We experience our body not as a set of fragmented parts, but rather as a single entity. How does this perception of owning an entire body arise? At the heart of this problem lies the necessity of binding together visual, tactile, and proprioceptive information from multiple body parts into a unitary multisensory percept of one's own whole body. Here, we addressed this question by measuring healthy participants' brain activity with functional magnetic resonance imaging (fMRI) as they experienced controlled changes in ownership of an entire body using the "body-swap" illusion paradigm [12]. This illusion is elicited when a participant observes tactile stimulation on the body of a mannequin from the point of view of the mannequin's head while feeling identical synchronous touches on his or her own body, which is out of sight.

We hypothesized that two basic processes would mediate ownership of an entire body. First, the self-attribution of individual body parts was expected to be mediated through integration of visual, tactile, and proprioceptive information in body-part-centered coordinates by neuronal populations in the ventral premotor and intraparietal cortices [3]. This prediction was based on neuroimaging studies investigating feelings of limb ownership [8, 9] and on neurophysiological studies in nonhuman primates revealing that these areas contain neurons that integrate visual, tactile, and proprioceptive information in reference frames centered on different parts of the body (e.g., the hand, arm, and head) [13–17].

Second, we hypothesized that the perceptual binding of owned body parts into a unified whole is supported by multisensory integration across body segments. This hypothesis was based on the observation that, during full-body illusion, the feeling of ownership spreads out from the stimulated body part to the rest of the (unstimulated) body [12]. We predicted that the underlying neural mechanism would be the visuosomatic integration across body segments, performed by special groups of multisensory neurons located in the premotor and intraparietal areas that have visuosomatic receptive fields extending across several body segments [14, 15, 18, 19], sometimes even encompassing the entire body [20].

To test the first hypothesis (above), we developed an fMRI-compatible setup to induce the body-swap illusion (see Supplemental Results and Supplemental Experimental Procedures available online) and performed two separate fMRI experiments. In the first experiment, involving 26 naive participants, we investigated the specific hypothesis that full-body ownership is associated with visuotactile integration in key multisensory regions, but only in the context of seeing a humanoid body [12]. To this end, we employed a two-by-two factorial design in which we systematically varied the type of object observed (humanoid body versus wooden object) and the timing of the visual and tactile stimuli (synchronous versus asynchronous) and computed the interaction term, which identified areas showing a greater effect of visuotactile synchrony in the context of seeing the humanoid body [8, 9, 12] (see Figure S1). In support of our hypothesis, we found significant activation in the right ventral premotor cortex (PMv) (54, 4, 34; $t = 3.41$; $p = 0.031$) (all coordinates reported are in MNI space), the left PMv (−60, 12, 28; $t = 3.76$; $p = 0.012$), and the left intraparietal sulcus (IPS) (−38, −48, 54; $t = 3.72$; $p = 0.014$) (Figure 1; Table S1). We also observed activation in the left putamen that did not reach significance after correction for multiple comparisons (−22, −8, 8; $t = 3.18$; $p < 0.001$, uncorrected). However, because this multisensory structure [21] was significantly activated in subsequent experiments, it is noteworthy to report here (Figure S2).

In the second fMRI experiment, we tested the hypothesis that the multisensory processes giving rise to the full-body illusion operate in body-centered reference frames [22, 23]. We compared conditions where the artificial body was presented in a similar location and orientation as the participant's real body (i.e., viewed from the first-person visual perspective

[3]These authors contributed equally to this work

*Correspondence: valeria.petkova@ki.se

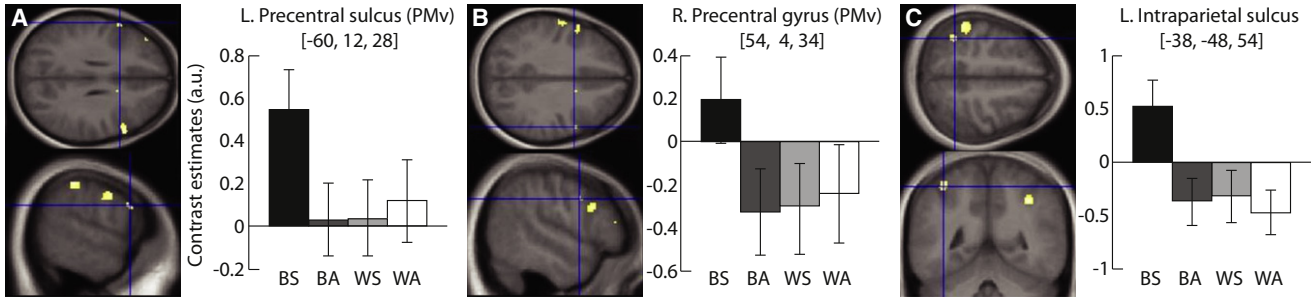

Figure 1. Activation during the Full-Body Illusion in Experiment 1: Stronger Effect of Visuotactile Synchrony When Observing the Mannequin

Activation maps corresponding to the interaction term in the factorial design (synchrony × human body), superimposed on a mean anatomical image for all 26 participants (threshold at $p < 0.001$, uncorrected for display purposes). The plots represent the contrast estimates (beta parameters of the general linear model) for the significant peaks ($p < 0.05$ after small volume correction) for the left and right ventral premotor area (A and B) and the left intraparietal sulcus (C). B and W stand for body and wood, respectively; S and A stand for synchronous and asynchronous visuotactile stimulation, respectively. Error bars represent the standard error. For further details, see Figure S1 and Table S1.

in near-personal space) or when the body was lying directly opposite the participant (i.e., viewed from the third-person visual perspective in far extrapersonal space) (Figure S1). Accordingly, in a new group of 20 naive participants, we manipulated the visual perspective (first-person versus third-person) and the timing of touches (synchronous versus asynchronous) in a two-by-two factorial design. We examined the interaction term, which in this analysis identifies enhanced responses to visuotactile synchronicity when the body is seen from the first-person perspective in near-personal space. In agreement with our hypothesis, we observed significant interaction in the right PMv (62, 2, 26; $t = 3.61$; $p = 0.032$) and the left IPS (−46, −48, 58; $t = 3.33$, $p = 0.041$) and a statistical trend in the left PMv (−54, 20, 34; $t = 3.07$; $p = 0.001$, uncorrected) (Figure 2; Table S1). In addition, we found significant activity in the left putamen matching that observed in the first experiment (−26, −8, 6; $t = 3.60$; $p = 0.021$) (Figure S2).

Importantly, in both experiments, the levels of activity in key multisensory areas associated with body-centered visuosomatic integration correlated with the degree of subjectively experienced full-body ownership. In the first experiment, the blood oxygen level-dependent (BOLD) response in the left PMv was significantly related to the strength of the illusion as rated by the participants directly after the scans (regression analysis; see Supplemental Experimental Procedures) (−60, 16, 16; $t = 3.70$; $p = 0.05$) (Figure 3A). In the second experiment, we found such significant relationships in the right PMv (44, 18, 34; $t = 4.09$; $p = 0.036$) and the left dorsal premotor cortex (PMd) (−42, 6, 48; $t = 3.98$; $p = 0.042$) (Figures 3B and 3C). In summary, the results from the two first experiments provide compelling evidence that the illusion of owning an entire body relies on body-part-centered integration of visual and somatic signals in multisensory areas.

Next, we focused on the central issue of how the feeling of ownership spreads from the site of stimulation to encompass the whole body, as is known to occur during the body-swap illusion [12]. In a third fMRI experiment, with a new group of 20 naive participants, we employed two complementary experimental designs to directly test the hypothesis that multisensory integration across body segments mediates the perceptual binding of owned body parts.

In the first design, we stimulated the right hand either when it was visually perceived as part of the mannequin's body or when the same hand was presented in isolation, i.e., as a detached limb. On the basis of previous work on the rubber-hand illusion [24–26] and our own pilot experiments, we hypothesized that strong ownership of a limb would only be present when the limb was perceived to be part of a body and that, in this context, the self-attribution of the limb would spread to the rest of the body. Thus, in a two-by-two factorial design, we manipulated the integrity of the body and the right hand (attached versus detached) and the timing of the touches

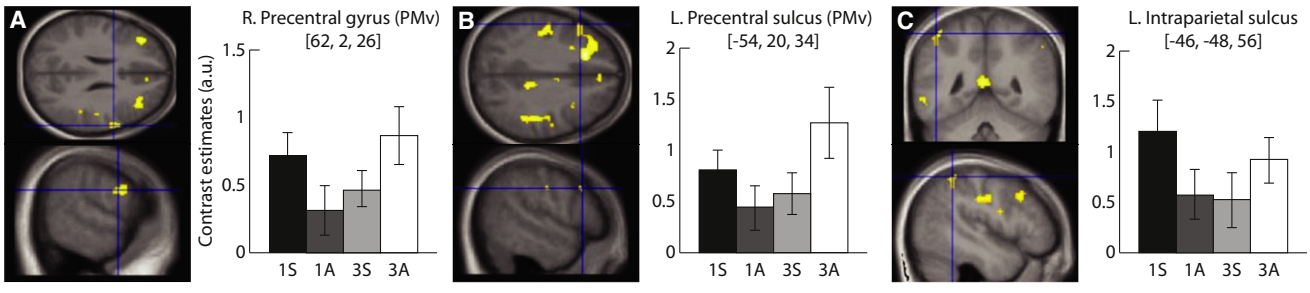

Figure 2. Activation during the Full-Body Illusion in Experiment 2: Stronger Effect of Visuotactile Synchrony When Viewing the Body from the First-Person Perspective

Activation maps corresponding to the interaction term in the factorial design (synchrony × first-person perspective), superimposed on a mean anatomical image for all 20 participants ($p < 0.001$, uncorrected for display purposes). The plots represent the contrast estimates (beta parameters of the general linear model) for the significant peaks of activation in the right PMv (A) and left IPS (C) ($p < 0.05$ after small volume correction) and activity in the left PMv (B) ($p < 0.001$, uncorrected), which did not reach significance after correction for multiple comparisons. 1 and 3 stand for first- and third-person perspective, respectively; S and A stand for synchronous and asynchronous visuotactile stimulation, respectively. Error bars represent the standard error. For activations in the putamen, see Figure S2.

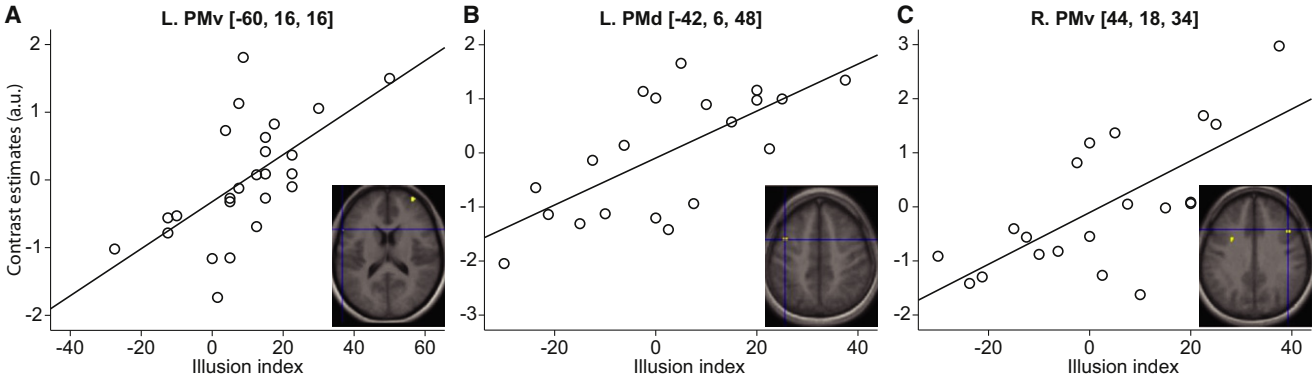

Figure 3. The Strength of the Illusion Is Linearly Related to the Amplitude of the BOLD Signal in the Premotor Cortex in Experiments 1 and 2

Participants who reported stronger self-attribution of the mannequin in the postscan questionnaires also exhibited greater illusion-related BOLD signal response (interaction term in the factorial designs) in the premotor cortex in study 1 (A) and study 2 (B and C) ($p < 0.05$ after small volume correction; activation maps have a threshold of $p < 0.001$, uncorrected for display purposes).

(synchronous versus asynchronous). Critically, we observed significant activations in the left PMv (−48, 6, 32; t = 3.60; p = 0.020) and the left IPS (−42, −38, 46; t = 4.00; p = 0.006) that reflected a greater effect of visuotactile synchrony when the arm was attached to the body (interaction term in the factorial design) (Figure 4A; Table S1). Again, weaker responses were noted in the left putamen (−26, 4, −8; t = 3.97; p = 0.001, uncorrected) (Figure S2). These results show that the perceived limb-body integrity augments the premotor-intraparietal activation, supporting our hypothesis that neural computations in these areas reflect the spread of ownership across connected body parts (see above).

In the second design, we compared conditions in which we elicited the illusion by stimulating either the hand or the abdomen (compared against the corresponding asynchronous controls). We hypothesized that the neuronal populations that mediate full-body ownership by integrating multisensory information across body parts should be active irrespective of the body part stimulated (i.e., body part independent). Consistent with this hypothesis, we found a significant cluster of voxels in the left PMv that was active when the body-swap illusion was triggered by stimulation in both the abdomen and the hand (−50, 0, 30; t = 3.39; p = 0.030; conjunction analysis; Figure 4B).

This premotor activation could, however, reflect either a genuine full-body ownership representation (i.e., one that could be implemented by multisensory neurons with receptive fields extending to multiple body segments) or activation of distinct groups of neurons with receptive fields restricted to individual body segments intermingled within the same voxels. To examine this effect, we applied multivoxel pattern analysis, a technique sensitive to fine-grained spatial patterns and subvoxel information [27, 28]. We used local multivariate brain mapping [29] to search for multivoxel patterns in the left ventral premotor cortex where classifiers trained to decode the illusion induced by stimulating the abdomen (i.e., distinguish synchronous from asynchronous visuotactile stimulation of the abdomen) could successfully generalize to decode patterns of activity reflecting the illusion when the hand was stimulated (i.e., distinguish synchronous from asynchronous visuotactile stimulation of the hand). We found such voxels in all 20 subjects (Figure 4C; $p < 0.05$, uncorrected, permutation test with 999 iterations; see Supplemental Experimental Procedures for details), and the decoding accuracy at the group level was significantly above chance, as was the reverse generalization from hand to abdomen ($p < 0.05$, permutation test, 999 iterations; Figure S3). Crucially, these multivoxel patterns were specific to the full-body illusion, because the classifiers failed to generalize when the hand was not attached to the mannequin's body (Figure 4C). Importantly, no body-part-specific patterns were identified within this body-part-independent section of the premotor cortex, because the classifiers failed to distinguish between synchronous visuotactile stimulation of the hand and abdomen. Taken together, these results suggest that activity in the left ventral premotor cortex reflects ownership generalized to the whole body.

Finally, it is noteworthy that the activations related to stimulation of the hand or the abdomen overlapped only partly (Figure 4B), allowing us to identify sections in the premotor and intraparietal cortices that selectively responded to visuotactile stimulation to one body part only (body part specific). This result suggests the existence of groups of multisensory cells in the human brain with receptive fields restricted to individual body parts, in analogy to the brains of nonhuman primates [13–19, 30, 31]. Given our results, we questioned whether we could detect ownership-related modulation in the BOLD signal in these body-part-specific regions, in line with the psychological observation that ownership spreads from the stimulated body part to the rest of the body [12]. Interestingly, we observed augmentation of the BOLD signal in abdomen-specific cortical sections of both the ventral premotor and intraparietal cortices, especially when the stimulation was applied to the hand attached to the mannequin's body (interaction contrast; $p < 0.001$, uncorrected) (Figure 4D). We speculate that this effect is a sign of the facilitation of the integration of visual and proprioceptive information in abdomen-specific neuronal populations during the full-body illusion, driven by the integration of visual, tactile, and proprioceptive signals from the stimulated hand. Although the present experiment was not designed to test specific hypotheses about the mechanism producing this modulatory effect, we speculate that corticocortical connections within the premotor-intraparietal system [30] or horizontal connections within the ventral premotor cortex may mediate it.

In summary, two major findings have been revealed in the present study. First, we found activation in the premotor

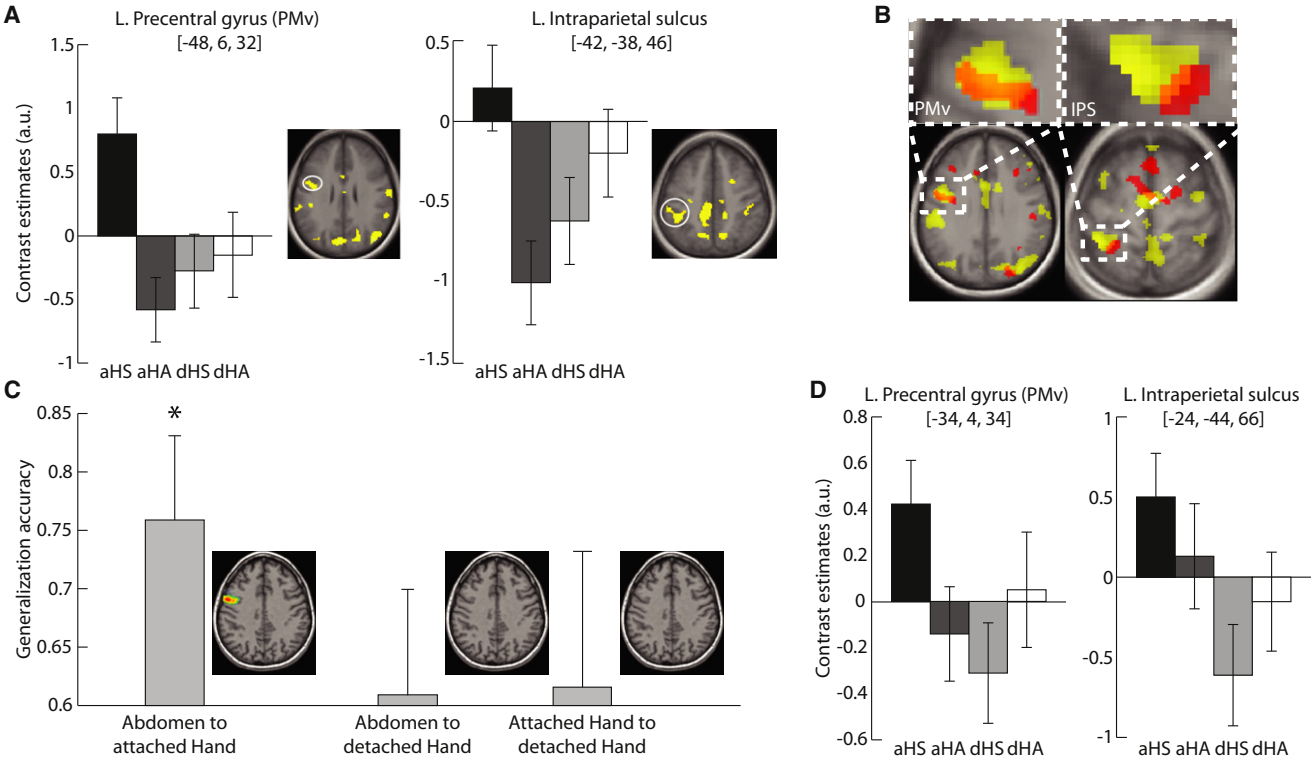

Figure 4. Activation Specific to Full-Body Ownership in Experiment 3

(A) The activation in the left ventral premotor cortex (PMv) and left intraparietal sulcus (IPS) related to the full-body illusion was significantly augmented when the hand was perceived as part of the body ($p < 0.05$, corrected). aH and dH indicate whether the hand was attached or detached, respectively; S and A stand for synchronous and asynchronous visuotactile stimulation, respectively. Error bars in (A) and (D) represent the standard error. Activation maps in (A) and (B) are at a threshold of $p < 0.001$, uncorrected for display purposes.

(B) Active voxels in the left PMv and IPS can be classified as body part specific (hand in yellow, abdomen in red) or body part independent (orange, conjunction of hand and abdomen).

(C) Multivoxel patterns in the left PMv reflect ownership generalized across body parts; classifiers trained to decode the illusion (synchronous versus asynchronous visuotactile stimulation) induced on the abdomen could successfully decode the illusion evoked when touching the hand. This generalization failed when the hand was perceived as a detached limb, both when the classifiers were trained on the abdomen and on the attached hand. The brain map shows voxels with a decoding accuracy significantly above chance in one representative subject ($p < 0.05$, permutation test, 999 iterations, uncorrected). The bar charts and error bars represent group average peak decoding accuracies ($n = 20$) and standard deviations, respectively. *$p < 0.05$ for group decoding accuracy, permutation test, 999 iterations. The reversed generalization was also confirmed (Figure S3).

(D) Abdomen-specific sections of the left PMv and IPS display an increase in the BOLD signal when the full-body illusion is driven by visuotactile stimulation on the hand, but only when it is attached to the mannequin's body ($p < 0.001$, uncorrected).

cortex, intraparietal cortex, and putamen that mirrored the perceptual rules of the full-body ownership illusion [12, 22, 23]. The anatomical locations of these activations were in regions that are well-known multisensory processing nodes in the primate brain (see Supplemental Discussion). Consistent activations across the three experiments were found only in these multisensory regions, and not in other parts of the brain, even when we lowered the statistical threshold ($p < 0.001$, uncorrected; see Supplemental Discussion). Our results thus suggest that the integration of visual, tactile, and proprioceptive information in body-part-centered reference frames represents a basic neural mechanism underlying the feeling of ownership of entire bodies. This finding generalizes existing models of limb ownership to the case of the entire body [3, 7, 10, 32]. Second, our results show that, in addition to body-part-specific multisensory integration, a process exists that mediates the perceptual binding of the parts into a unified percept of a whole owned body. Activation in the key multisensory areas (ventral premotor cortex, intraparietal cortex, and putamen) increased when the stimulated body part was attached to a body, as compared to when it was detached, showing that the context of integrity between body segments facilitates ownership of these parts. Furthermore, in the left ventral premotor cortex, we found an active area and multivoxel patterns of activity that reflected full-body ownership irrespectively of which body part was simulated. The latter two findings can best be explained by a parsimonious model in which the unitary experience of owning a whole body is produced by neuronal populations in the ventral premotor cortex, and possibly in other multisensory areas, that integrate multisensory information across body parts. This type of multisensory integration could be ideally implemented by neurons with large visual, tactile, and proprioceptive receptive fields extending over multiple body segments [15, 19, 33, 34].

Supplemental Information

Supplemental Information includes three figures, one table, Supplemental Results, Supplemental Discussion, and Supplemental Experimental Procedures and can be found with this article online at doi:10.1016/j.cub.2011.05.022.

Acknowledgments

This work was funded by the European Research Council, the Human Frontier Science Program, the Swedish Foundation for Strategic Research, Söderbergska Stiftelsen, and the James S. McDonnell Foundation. The first imaging experiment was conducted as part of the PRESENCCIA project, a European Union-funded project under the Information Society Technologies Program. We thank Nikolaus Weiskopf and Oliver Josephs (Functional Imaging Laboratory, University College London) for early MRI compatibility tests of the head-mounted display system.

Received: February 7, 2011
Revised: April 1, 2011
Accepted: May 11, 2011
Published online: June 16, 2011

References

1. Bermudez, J.L., Marcel, A., and Eilan, N. (1998). The Body and the Self (Cambridge, MA.: MIT Press).
2. Blanke, O., and Metzinger, T. (2009). Full-body illusions and minimal phenomenal selfhood. Trends Cogn. Sci. *13*, 7–13.
3. Ehrsson, H.H. (2011). The concept of body ownership and its relationship to multisensory integration. In The Hand Book of Multisensory Processes, B. Stein, ed. (Cambridge, MA: MIT Press).
4. Graziano, M., and Botvinick, M. (2002). How the brain represents the body: Insights from neurophysiology and psychology. In Common Mechanisms in Perception and Action: Attention and Performance XIX, W. Prinz and B. Hommel, eds. (Oxford: Oxford University Press), pp. 136–157.
5. Gallagher, S. (2005). How the Body Shapes the Mind (Oxford: Oxford University Press).
6. Merleau-Ponty, M. (2005). Phenomenology of Perception (London: Routledge Classics).
7. Botvinick, M., and Cohen, J. (1998). Rubber hands 'feel' touch that eyes see. Nature *391*, 756.
8. Ehrsson, H.H., Holmes, N.P., and Passingham, R.E. (2005). Touching a rubber hand: Feeling of body ownership is associated with activity in multisensory brain areas. J. Neurosci. *25*, 10564–10573.
9. Ehrsson, H.H., Spence, C., and Passingham, R.E. (2004). That's my hand! Activity in premotor cortex reflects feeling of ownership of a limb. Science *305*, 875–877.
10. Makin, T.R., Holmes, N.P., and Ehrsson, H.H. (2008). On the other hand: Dummy hands and peripersonal space. Behav. Brain Res. *191*, 1–10.
11. Tsakiris, M., and Haggard, P. (2005). The rubber hand illusion revisited: Visuotactile integration and self-attribution. J. Exp. Psychol. Hum. Percept. Perform. *31*, 80–91.
12. Petkova, V.I., and Ehrsson, H.H. (2008). If I were you: Perceptual illusion of body swapping. PLoS ONE *3*, e3832.
13. Avillac, M., Deneve, S., Olivier, E., Pouget, A., and Duhamel, J.-R. (2005). Reference frames for representing visual and tactile locations in parietal cortex. Nat. Neurosci. *8*, 941–949.
14. Rizzolatti, G., Scandolara, C., Matelli, M., and Gentilucci, M. (1981). Afferent properties of periarcuate neurons in macaque monkeys. II. Visual responses. Behav. Brain Res. *2*, 147–163.
15. Fogassi, L., Gallese, V., Fadiga, L., Luppino, G., Matelli, M., and Rizzolatti, G. (1996). Coding of peripersonal space in inferior premotor cortex (area F4). J. Neurophysiol. *76*, 141–157.
16. Graziano, M.S. (1999). Where is my arm? The relative role of vision and proprioception in the neuronal representation of limb position. Proc. Natl. Acad. Sci. USA *96*, 10418–10421.
17. Graziano, M.S., Hu, X.T., and Gross, C.G. (1997). Visuospatial properties of ventral premotor cortex. J. Neurophysiol. *77*, 2268–2292.
18. Duhamel, J.-R., Colby, C.L., and Goldberg, M.E. (1998). Ventral intraparietal area of the macaque: Congruent visual and somatic response properties. J. Neurophysiol. *79*, 126–136.
19. Graziano, M.S., and Gandhi, S. (2000). Location of the polysensory zone in the precentral gyrus of anesthetized monkeys. Exp. Brain Res. *135*, 259–266.
20. Graziano, M.S., Cooke, D.F., and Taylor, C.S.R. (2000). Coding the location of the arm by sight. Science *290*, 1782–1786.
21. Graziano, M.S., and Gross, C.G. (1993). A bimodal map of space: Somatosensory receptive fields in the macaque putamen with corresponding visual receptive fields. Exp. Brain Res. *97*, 96–109.
22. Petkova, V.I., Khoshnevis, M., and Ehrsson, H.H. (2011). The perspective matters! Multisensory integration in ego-centric reference frames determines full body ownership. Front. Psychol. *2*, 35. 10.3389/fpsyg.2011.00035.
23. Slater, M., Spanlang, B., Sanchez-Vives, M.V., and Blanke, O. (2010). First person experience of body transfer in virtual reality. PLoS ONE *5*, e10564.
24. Costantini, M., and Haggard, P. (2007). The rubber hand illusion: Sensitivity and reference frame for body ownership. Conscious. Cogn. *16*, 229–240.
25. Lloyd, D.M. (2007). Spatial limits on referred touch to an alien limb may reflect boundaries of visuo-tactile peripersonal space surrounding the hand. Brain Cogn. *64*, 104–109.
26. Pavani, F., Spence, C., and Driver, J. (2000). Visual capture of touch: Out-of-the-body experiences with rubber gloves. Psychol. Sci. *11*, 353–359.
27. Haynes, J.-D., and Rees, G. (2005). Predicting the stream of consciousness from activity in human visual cortex. Curr. Biol. *15*, 1301–1307.
28. Kamitani, Y., and Tong, F. (2005). Decoding the visual and subjective contents of the human brain. Nat. Neurosci. *8*, 679–685.
29. Björnsdotter, M., Rylander, K., and Wessberg, J. (2011). A Monte Carlo method for locally multivariate brain mapping. Neuroimage *56*, 508–516.
30. Rizzolatti, G., Luppino, G., and Matelli, M. (1998). The organization of the cortical motor system: New concepts. Electroencephalogr. Clin. Neurophysiol. *106*, 283–296.
31. Avillac, M., Ben Hamed, S., and Duhamel, J.-R. (2007). Multisensory integration in the ventral intraparietal area of the macaque monkey. J. Neurosci. *27*, 1922–1932.
32. Tsakiris, M. (2010). My body in the brain: A neurocognitive model of body-ownership. Neuropsychologia *48*, 703–712.
33. Rizzolatti, G., Scandolara, C., Matelli, M., and Gentilucci, M. (1981). Afferent properties of periarcuate neurons in macaque monkeys. I. Somatosensory responses. Behav. Brain Res. *2*, 125–146.
34. Iwamura, Y. (1998). Hierarchical somatosensory processing. Curr. Opin. Neurobiol. *8*, 522–528.

Current Biology, Volume *21*

Supplemental Information

From Part- to Whole-Body Ownership

in the Multisensory Brain

Valeria I. Petkova, Malin Björnsdotter, Giovanni Gentile, Tomas Jonsson, Tie-Qiang Li, and H. Henrik Ehrsson

Inventory of Supplemental Information

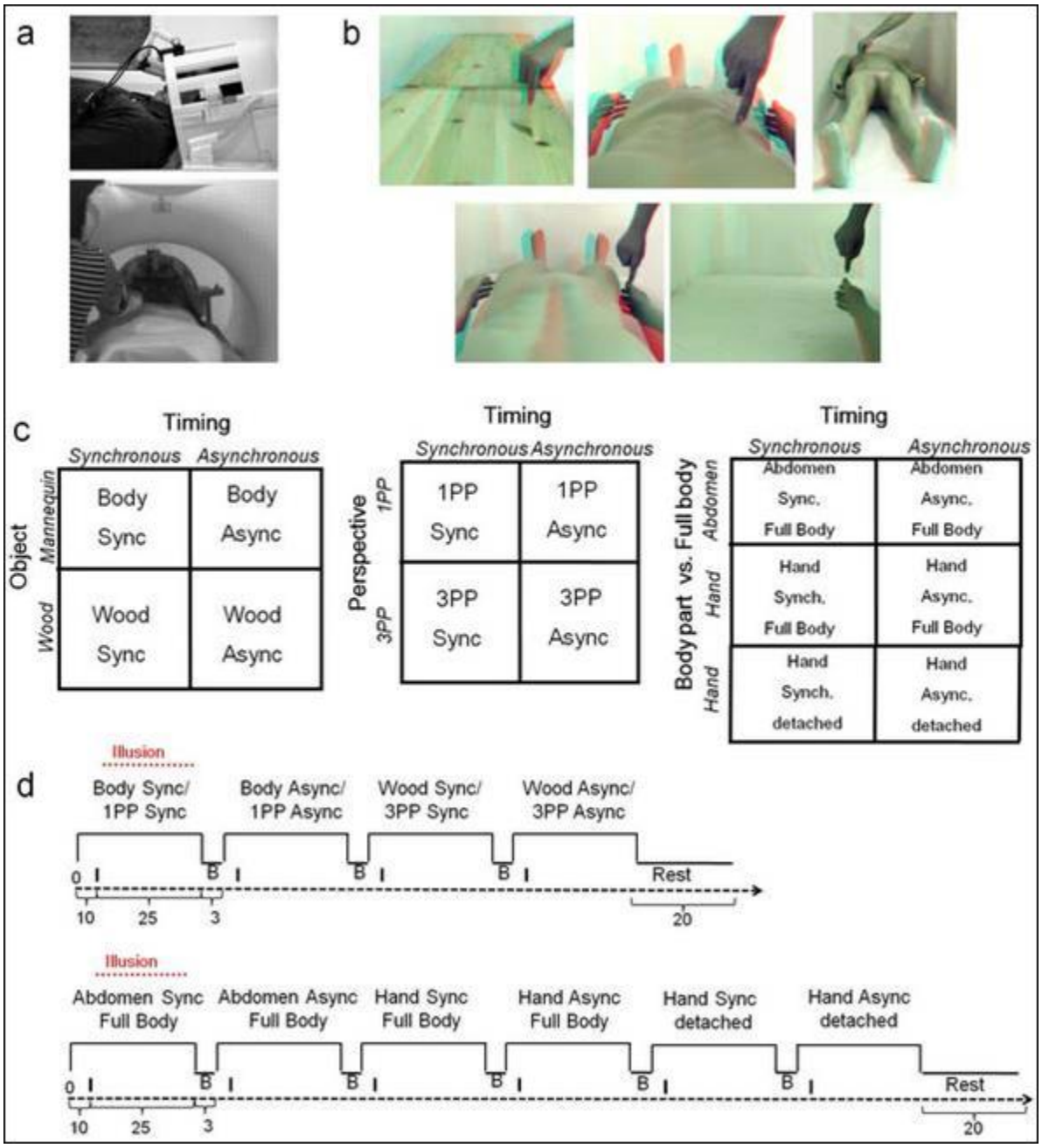

Figure S1. Experimental Setup and Factorial Designs Used in the fMRI Experiments

(A) The position of the MR compatible head-mounted displays in front of the participant's head (above), and the position of the experimenter while applying tactile stimulation (below).

(B) Snapshots of the original video stimuli used in the different experimental conditions. The red and blue image duplication is due to the 3D video cameras used to produce the video recordings. Red and blue filters were glued to the goggle screens to provide the participants with high-quality 3D images of the visual stimuli.

(C) The factorial designs in all three experiments.

(D) The timing sequences used for the experiments.

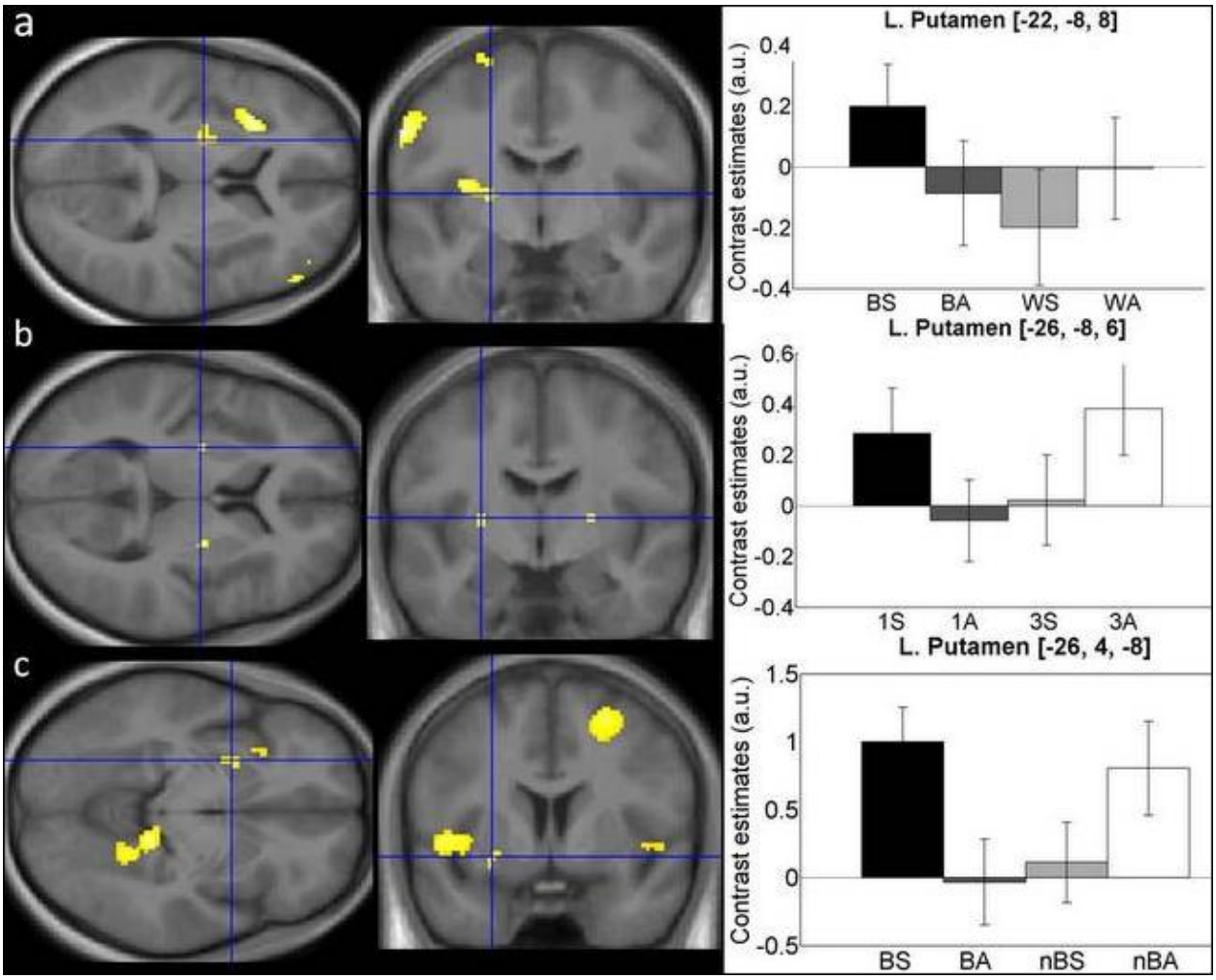

Figure S2. Activation in the Putamen during the Full-Body Illusion (Studies 1, 2, and 3)

(A) The left putamen revealed a BOLD-signal increase, especially when the participants perceived synchronized visuotactile stimulation applied to the body of the mannequin ($p < 0.001$, uncorrected) (interaction effect; study 1).

(B) Activity in the left putamen related to the body swap illusion reflected a greater effect of visuotactile synchrony when the mannequin was viewed from the first-person compared with the third-person perspective ($p < 0.05$, corrected) (interaction effect; study 2).

(C) Activation in the left putamen elicited by synchronized visuotactile stimulation applied to the hand was stronger when it was visually attached to the body than when it was presented as a detached limb ($p < 0.001$, uncorrected) (interaction effect, study 3). All activation maps are at a threshold of $p < 0.001$, uncorrected for display purposes.

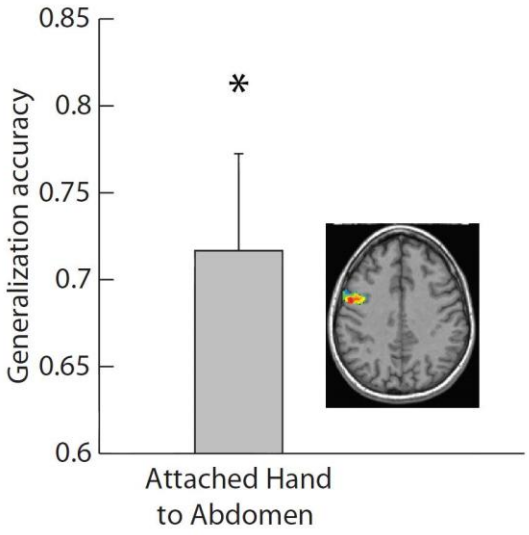

Figure S3. Reversed Generalization

Within the voxels where classifiers trained to decode the illusion induced on the abdomen successfully could decode the illusion evoked when touching the hand, the reverse was also confirmed. Individual peak decoding accuracy averages resulting from classifiers trained on the attached hand condition and tested on the abdomen condition was significantly above chance ($p < 0.05$, permutation test, 999 iterations). The brain map shows voxels with a decoding accuracy significantly above chance in one representative subject ($p < 0.05$, permutation test, 999 iterations, uncorrected).

Table S1. All brain regions (peaks) that revealed significant activation at p=0.001 (uncorrected) in experiments #1 and #2 are listed. FWE-corrected p-values are reported for regions that survived the correction for multiple comparisons in anatomically predefined regions (small volume corrections). [a, b] and [c] denotes the study of origin for the MNI coordinates used to perform small volume corrections. Peaks without [a, b] or [c] survived whole brain FWE-correction.

STUDY 1

ANATOMICAL REGION	peak p(FWE-cor)	peak T	MNI x,y,z {mm}
INTERACTION ANALYSIS			
PARIETAL LOBE			
L. Intraparietal Sulcus[a]	0.014	3.72	-38, -48, 54
L. Supramarginal Gyrus	-----	3.90	-60, -34, 48
R. Intraparietal Sulcus	-----	4.03	34, -46, 42
L. Postcentral Gyrus	-----	3.76	-60, -6, 38
INSULAR CORTEX			
L. Anterior Insula	-----	4.17	-30, 18, 10
L. Insula	-----	3.60	-34, -6, 12
FRONTAL LOBE			
L. Precentral Sulcus (PMv)[b]	0.012	3.76	-60, 12, 28
R. Precentral Gyrus (PMv) [b]	0.031	3.41	54, 4, 34
L. Left Middle Frontal Gyrus	-----	4.02	-44, 42, 24
R. Inferior Frontal Gyrus	-----	4.18	52, 40, 12
R. Inferior Frontal Gyrus	-----	3.86	56, 16, 28
SUBCORTICAL REGIONS			
L. Putamen	-----	3.18	-22, -8, 8
REGRESSION ANALYSIS			
FRONTAL LOBE			
L. Precentral Sulcus (PMv)[a]	0.05	3.70	-60, 16, 16
R. Superior Medial Gyrus	-----	4.75	8, 26, 60
R. Superior Frontal Gyrus	-----	4.07	34, 60, 16
R. Inferior Frontal Gyrus	-----	5.03	54, 34, 4
CEREBELLUM			
R. Cerebellum Lobule VIIa Crus I	-----	3.52	36,-78,-36

STUDY 2

ANATOMICAL REGION	peak p(FWE-cor)	peak T	MNI x,y,z {mm}
INTERACTION ANALYSIS			
PARIETAL LOBE			
L. Intraparietal Sulcus[c]	0.041	3.33	-46, -48, 56
R. Postcentral Sulcus	------	3.65	44, -28, 38
L. Postcentral Gyrus	------	3.26	-44, -22, 34
R. Postcentral Gyrus	------	3.48	46, -14, 30
L. Retrosplenial Cortex	------	3.76	-2, -46, 10
FRONTAL LOBE			
R. Precentral Gyrus (PMv)[b]	0.002	3.61	62, 2, 26
L. Precentral Sulcus (PMv)	------	3.07	-54, 20, 34
L. Middle Cingulate Cortex	------	3.74	-4, -22, 44
L. Middle Cingulate Cortex	------	3.64	-2, -14, 44
R. Anterior Cingulate Cortex	------	4.10	6, 46, 18
L. Superior Frontal Gyrus	------	3.52	-20, 18, 54
L. Superior Frontal Gyrus	------	4.58	-18, 26, 36
L. Middle Frontal Gyrus	------	4.25	-30, 10, 50
R. Middle Frontal Gyrus	------	3.54	32, 10, 48
R. Middle Frontal Gyrus	------	3.40	32, 32, 26
L. Inferior Frontal Gyrus	------	3.53	-38, 34, 26
L. Superior Medial Gyrus	------	3.36	-12, 42, 26
R. Superior Medial Gyrus	------	4.14	8, 38, 42
R. Mid Orbital Gyrus	------	3.73	6, 58, -6
SUBCORTICAL REGIONS			
L. Putamen[c]	0.021	3.60	-26, -8, 6
R. Putamen	------	3.80	24, -8, 8
REGRESSION ANALYSIS			
TEMPORAL LOBE			
L. Middle Temporal Gyrus	------	4.72	-50, -42, -4
FRONTAL LOBE			
L. Precentral Sulcus (PMd)[a]	0.042	3.98	-42, 6, 48
R. Precentral Sulcus (PMv)[a]	0.036	4.09	44, 18, 34
L. Middle Frontal Gyrus	------	5.76	-30, 8, 32
L. Inferior Frontal Gyrus	------	4.46	-44, 30, -10

L. Superior Frontal Gyrus	------	4.69	-14, 36, 38
R. Anterior Cingulate Cortex	------	5.68	8, 48, 20
R. Inferior Frontal Gyrus	------	4.22	44, 24, -10
CEREBELLUM			
R. Cerebellum Lobule IX	------	4.53	8, -56, -38
R. Cerebellum Lobule VIIa Crus I	------	3.87	24, -74, -28
L. Cerebellum Lobule VIIa Crus II	------	3.74	-26, -74, -32
SUBCORTICAL REGIONS			
L. Thalamus	------	6.10	-16, -18, 12
R. Putamen	------	4.58	30, 10, 4

STUDY 3

ANATOMICAL REGION	**peak p(FWE-cor)**	**peak T**	**MNI x,y,z {mm}**
INTERACTION ANALYSIS			
OCCIPITAL LOBE			
L. Cuneus	-----	4.83	-8, -76, 24
L. Anterior Calcarine Sulcus/Isthmus	-----	3.76	-4, -56, 8
R. Parieto-Occipital Fissure	-----	4.73	16, -64, 16
L. Parieto-Occipital Fissure	-----	4.07	-16, -62, 6
R. Isthmus	-----	4.58	14, -38, -6
L. Isthmus	-----	4.42	-12, -44, 2
R. Superior Occipital Gyrus	-----	3.69	20, -100, 4
R. Superior Occipital Gyrus	-----	4.29	24, -98, -4
L. Supperior Occipital Gyrus	-----	3.74	-20, -100, -8
R. Middle Occipital Gyrus	-----	4.37	42, -78, 28
PARIETAL LOBE			
R. Postcentral Gyrus	-----	4.93	30, -34, 68
R. Postcentral Sulcus	-----	4.02	54, -28, 52
R. Postcentral Gyrus	-----	3.49	14, -36, 74
L. Postcentral Gyrus	-----	4.39	-24, -26, 74
L. Postcentral Sulcus	-----	4.02	-40, -36, 62
L. Intraparietal Sulcus[a]	0.006	4.00	-42, -38, 46
R. Supramarginal Gyrus	-----	3.73	58, -44, 26
R. Supramarginal Gyrus	-----	3.47	64, -20, 44
L. Supramarginal Gyrus	-----	3.76	-68, -34, 26
L. Inferior Parietal Gyrus	-----	3.63	-42, -48, 34
R. Parietal Operculum	-----	4.79	40, -32, 20

R. Precuneus	-----	3.81	10, -62, 48
INSULAR CORTEX			
R. Circular Insular Sulcus	-----	3.58	40, -14, -8
L. Anterior Insula	-----	4.00	-46, 6, 0
TEMPORAL LOBE			
R. Superior Temporal Gyrus	0.018	5.35	54, -18, 6
L. Superior Temporal Gyrus	-----	4.03	-44, -18, -2
R. Inferior Temporal Gyrus	-----	3.80	48, -48, -8
L. Inferior Temporal Gyrus	-----	4.13	-54, -58, -10
R. Parahippocampal Gyrus	-----	4.52	26, -30, -20
L. Superior Temporal Sulcus	0.037	5.12	-50, -76, 22
FRONTAL LOBE			
R. Precentral Gyrus (PMd)	-----	4.94	36, -12, 66
L. Precentral Gyrus (PMd)	-----	3.48	-30, -12, 56
L. Precentral Sulcus (PMv)[a]	0.020	3.60	-48, 6, 32
L. Precentral sulcus (PMv)	-----	3.61	-38, -6, 32
R. Superior Frontal Gyrus (SMA)	-----	3.49	8, -12, 72
L. Superior Frontal Gyrus (SMA)	-----	4.17	-2, -8, 58
R. Superior Frontal Gyrus	-----	3.69	16, 50, -8
R. Superior Frontal Sulcus	-----	4.17	26, 6, 56
L. Junction between Superior Frontal Sulcus and Precentral Sulcus	-----	3.99	-24, -6, 62
L. Superior Frontal Gyrus	-----	3.66	-22, 60, 10
R. Lateral Orbital Gyrus	-----	3.82	38, 58, 2
L. Middle Frontal Gyrus	-----	3.87	-30, 26, 36
R. Cingulate Gyrus	-----	3.46	2, -10, 30
L. Cingulate Gyrus	-----	3.58	-2, 12, 28
L. Cingulate Sulcus	-----	4.45	-12, -24, 42
L. Cingulate Gyrus	-----	3.45	-6, -2, 36
R. Medial Orbital Gyrus	-----	3.52	20, 32, -14
CEREBELLUM			
R. Cerebellum Lobule VI	-----	4.22	28, -48, -30
L. Cerebellum Lobule VI	-----	3.54	-26, -40, -28
L. Cerebellum Lobule VIIa Crus II	-----	3.68	-14, -86, -38
SUBCORTICAL REGIONS			
R. Putamen/Anterior Insula	-----	4.59	28, 18, -6
L. Putamen	-----	3.97	-26, 4, -8

---

[a]Small volume correction (10mm) around MNI coordinates reported in [1]
[b]Small volume correction (10mm) around MNI coordinates reported in [2]
[c]Small volume correction (10mm) around MNI coordinates reported in the first fMRI experiment in this study.

Supplemental Results

Reproducing the Body-Swap Illusion in the Scanner: Subjective and Objective Evidence

Before the fMRI experiments were conducted, we sought to ensure that the full-body ownership illusion [3] could be reproduced in the set-up adapted for fMRI. Hence, in two separate experiments, we tested whether a naive participant could experience the body-swap illusion when lying on a bed with their head tilted, watching videos of a mannequin being touched in synchrony or asynchrony with identical touches applied to their own body [3].

In the first experiment, we recruited twenty-five naive participants (18 females, mean age 26 years ± 4 SD). Each participant was positioned comfortably on a bed with their head supported in a forward-tilted position and was instructed to put on a set of head-mounted displays, which had identical fields of view (45 degrees in the horizontal plane) as those used in the fMRI studies. During the experiment, the participant watched a 3D video of a mannequin being touched. The body of the mannequin was perceived from the first person visual perspective of the participant; thus, it was in the location where normally one's own body would be perceived. We used the two key conditions from the previous report on the full-body ownership illusion [3], in which the participants felt touches on their bodies that were synchronous (condition #1) or asynchronous (condition #2) with the observed touches delivered to the body of the mannequin. At the end of each session, the participants were required to rate the degree of their agreement or disagreement with seven statements using a 7-point Likert scale [3]. Three statements captured the perceptual illusion of the mannequin's body being perceived as one's own body. Four statements served as controls [3]. The results from the questionnaires demonstrate that the participants experienced strong illusory self-attribution of the mannequin's body, as indicated by the significant interaction between the factors "Timing of visuotactile stimulation" (synchronous vs. asynchronous) and "Question type" (illusion vs. control) ($N = 25$, $p < 0.001$, $F(1, 24) = 32.747$, two-way 2x2 ANOVA).

In the second experiment, we used threat-evoked skin conductance responses to provide objective evidence for the illusory perception [3]. For this experiment, we invited thirteen new participants (5 females, 24 ± 3 years SD) and subjected them to one minute of either synchronous or asynchronous visuotactile stimulation as described above. Immediately after each session had ended, the participants saw a knife 'cutting' into the abdomen of the mannequin according to the previously published procedures [3]. The resulting changes of the Skin Conductance Responses (SCR) were recorded. Each condition was repeated three times in a pseudo-randomized order. The results showed that the synchronous condition was associated with a significantly greater threat-evoked SCR compared to the asynchronous condition ($N = 13$, $p = 0.023$, related samples Wilcoxon Signed Rank test). Thus, both the subjective and objective data showed that the body-swap illusion could be robustly reproduced when pre-recorded videos were used to trigger the visuotactile stimulation and when the participants lay on beds with the head in a tilted position.

Supplemental Discussion

The Premotor-Intraparietal-Putamen Circuits: Anatomy, Physiology, and Neuroimaging

The premotor cortex, the intraparietal cortex and the putamen are ideally suited to perform the complex multisensory integration required to produce the full-body illusion described here, as they are key nodes in the cortical pathways that integrate multisensory signals for the control of sensory-guided actions in body-part-centered reference frames [4, 5]. These regions receive anatomical projections from the early visual and somatic areas in the occipital and anterior parietal lobes [6, 7]. Numerous electrophysiological studies that have targeted these regions have described neurons in the ventral premotor cortex [8-10], the intraparietal cortex (areas MIP, VIP and LIP; medial, ventral and lateral intraparietal areas, respectively) [11-16] and the putamen [17] that respond to visual, tactile and proprioceptive stimulation. Crucially, neurons in these areas are known to have visual receptive fields (RFs) centered on a monkeys' head, face, neck, torso, shoulders, hands, arms or whole body [8, 10, 12, 18-20] that overlap considerably with the same neurons' tactile RFs. Furthermore, these visuotactile RFs are anchored to the specific limb or body part, so that when the limb or body part moves, the visual RFs of the bisensory neurons move along with it [8-10, 15, 17]. Recent fMRI studies suggest that the human premotor and intraparietal cortex integrate multisensory information from near-personal space in a fashion that is similar to the macaque brain. The human premotor cortex and intraparietal cortex respond to polymodal visual, tactile and auditory stimulation [21] and are activated during cross-modal visuotactile reaction time tasks [22, 23]. Of more direct relevance for the present investigations are the observations that the human premotor cortex [24, 25], intraparietal cortex [24, 25] and putamen [24] are activated when the own (real) arm is touched in full view and that these areas respond preferentially to visual stimulation in near-personal space [26, 27]. Furthermore, the human ventral premotor cortex, intraparietal cortex, putamen and inferior parietal cortex perform integration of visual and somatic signals in an additive or superadditative fashion [24]. Thus, the illusion-specific increases in the BOLD-signal in the ventral premotor cortex and the intraparietal sulcus fit well with the hypothesis that the sense of owning an entire body is produced by active neuronal populations that integrate visual, tactile and proprioceptive information in body-part-centered coordinates, within and across body segments, as discussed in the main text. Indeed, the BOLD response in these areas obeyed the temporal and spatial principles of multisensory integration; a positive effect of the synchronicity was only seen for visuotactile stimuli employed on a human body presented in an anatomically congruent position in near-personal space. This conclusion was further strengthened by the observation that stronger subjectively reported illusions yielded stronger multisensory effects in the premotor cortex (interaction effect in Experiments #1 and #2), which is a key node in these fronto-parietal [28-30] and fronto-striatal circuits [17]. Our data also suggest that both multisensory neurons with receptive fields restricted to single body parts and multisensory neurons with receptive fields extending over multiple body segments are involved in generating the full-body illusion. Support for the former comes from Experiment 3, where we found active fields in the ventral premotor cortex that showed body-part specificity that also displayed a modulation of the BOLD-signal related to the full-body illusion. Support for the involvement of multisensory neurons with large receptive fields comes from the findings of active premotor voxels that reflect the generalization of ownership across body parts and active clusters that do not show body-part specificity. The idea that the multisensory perception of one's own body is constructed by the same circuits that control object-directed

action [7] and defensive movements [31] fits well with the principle that the ultimate goal for multisensory integration is the production of adaptive behavior [32, 33].

Anatomical Specificity of the Activations

The activations reflecting the full-body illusion were specific to the premotor-intraparietal-putamen regions and were not seen in other brain areas. When we lowered the statistical threshold to $p < 0.001$ (uncorrected), we did observe some activations in the anterior and posterior insula (see Supplementary Table 1), but these peaks were not reproducible across the studies and were therefore deemed unreliable. Further, we could not find any significant increases in activation in the right temporo-parietal junction (TPJ) associated with the present illusion. Although we did observe a statistical trend for activation in the right supramarginal gyrus region in the third experiment [58, -44, 26; $p < 0.001$; interaction term in the factorial design], no such trends was observed in Experiments #1 or #2. Rather, in the second fMRI experiment, we observed a significant main effect of asynchronous visuotactile stimulation in the left superior temporal sulcus, an area that is considered to be part of the TPJ. Thus, the TPJ could be signalling mismatches in multisensory stimulation, which would be consistent with earlier fMRI studies describing responses in this region during violations of multisensory predictions [34, 35]. However, we found no evidence that this asynchrony response was related to the illusion, as it was not modulated by the visual perspective, was not correlated (positively or negatively) with the strength of the illusion and was not reproduced in the first or the third fMRI experiment. On the basis of the association between the TPJ and neurological out-of-body experiences, it was suggested that this region could be involved in the integration of vestibular signals with other body signals and the mapping of ego-centric visuotactile representations of the body with respect to (far) extrapersonal space (allocentric coordinates) [36, 37]. If these hypotheses are correct, it is not surprising that we did not observe any activation in this area, as the present illusions did not involve any vestibular sensations or perceived changes in self-location in allocentric space. Thus, a possible interpretation that is consistent with the existing literature is that ownership of the body is computed in premotor-intraparietal-striatal circuits and that a sense of self-location in the world and orientation in the gravity field requires the TPJ region.

Illusions, Perception, Attention

In the present study, we used the classical approach of psychology to study illusions to reveal the basic mechanisms that mediate perception. Indeed, it is difficult, if not impossible, to investigate the feeling of body ownership by means other than the use of perceptual illusions because the body is ‘always there’ [38]. A general limitation of this approach, however, is that there is always the risk that the brain activation seen during the illusion could reflect unspecific effects related to attention or arousal when having an unusual perceptual experience [39]. Nevertheless, in the present study, there are several reasons why the activations in the premotor cortex, the intraparietal sulcus and the putamen are likely to reflect multisensory perception mechanisms related to body ownership rather than unspecific effects related to attention, expectation or arousal. First, the participants were not required to perform any active cognitive or motor tasks but were simply instructed to look at the scene presented in the MR-compatible goggles. This step was performed to exclude the possibility that any potential task-selective or task-preparatory activity could confound the activation maps. Second, all participants were naïve to the purpose of the experiment and hence did not have any expectations about what they would experience under

the different conditions. Third, we excluded the first 10 seconds of each stimulus epoch from analysis. This exclusion eliminates any putative increase in brain activity associated with the initial allocation of spatial attention or stimulus-driven attention related to a sudden change in the sensory environment. Forth, the main conclusions were based on the converging results from inspecting the interaction term in the factorial designs of the three separate experiments. In this type of contrast, only 'super-additive' responses are detected when contrasting the four conditions, which effectively controls for all low-level features of the stimuli and for moderate changes in states of attention. In line with this, no significant interaction effects were observed in, for example, early sensory areas. Fifth, the activity reported in the present study is specific to the particular perceptual experience of the full body ownership illusion and is not seen in other types of body illusions (i.e., as in refs. [40, 41]). Sixth, when people observe their own real body parts being touched, the activations in the ventral premotor cortex, intraparietal cortex and putamen occur in very similar parts as those activations during the body-swap illusion [24]. Taken together, these arguments suggest that the present illusion-related activations reflect multisensory processing related to the sense of ownership of the artificial body.

Supplemental Experimental Procedures

Participants

A total of 66 healthy participants were recruited. The study consisted of three separate fMRI experiments. In the first experiment, we invited a group of twenty-six participants (12 female; aged 20 to 36 years); a group of twenty naïve participants were tested in the second experiment (7 female; aged 19 to 40 years), and another group of twenty participants was recruited for the third imaging experiment (5 female; aged 20 to 59 years). All participants were naïve to the specific purposes of the study, and none of them participated in two or more experiments. The Ethical Review Board of Karolinska Institutet approved the experimental protocol, and written informed consent was obtained from each participant.

Imaging Experiments

Positioning of Participants and MRI-Compatible HMDs

During the brain scans, each subject lay comfortably in a supine position on the MRI table with her head tilted at approximately 25 degrees. 3D video recordings of the visual stimuli were presented on MR-compatible head-mounted displays (HMDs; Nordic Neurolab, Bergen, Norway) positioned in front of the participants' eyes and controlled by Presentation (Version 13.1, Neurobehavioral Systems, Inc., www.neurobs.com) (Figure S1a). The 3D videos were recorded in a separate session before the fMRI experiments using a red/blue stereoscopic camera (novo Minoru, Salford, United Kingdom). As this process required separate red and blue filters to produce the stereoscopic effect, red and blue filters were glued in front of the left and right displays of the HMDs, respectively. In separate behavioral experiments, we verified that a robust full-body illusion can be induced using this set-up (see Supplemental Results and Figure S3)

Experimental Design and Conditions

In experiment 1, there were four experimental conditions organized in a two-by-two factorial design and a fifth baseline condition (Figure S1c, left panel). In the factorial design, we manipulated the factor *object* (wooden block vs. mannequin's body) and the factor *timing* (synchronous vs. asynchronous strokes applied to the two bodies). In the conditions Body Sync and Body Async, the participants looked at the body of a mannequin through the HMDs at a location and in an orientation similar to their own body in the scanner (Figure S1b, top left and middle panels). In the Wood Sync and Wood Async conditions, the body of the mannequin was replaced by a wooden object of similar size that was known to eliminate the illusion [3] (Figure S1b, top left panel). The tactile stimulations on the wooden block were applied at identical positions and distances from the cameras as in the conditions when the mannequin was used to ensure matched retinal stimulation. This design allowed us to identify areas that showed an effect of synchronous stimulation only when the mannequin was presented, which was performed by examining the interaction term in the factorial design (see main text).

In experiment 2, we similarly employed a two-by-two factorial design, but here we were interested in testing for an interaction that identified enhanced responses to visuotactile synchronicity when the body was seen from the first-person perspective (1PP) in near-personal space (Figure S1b, middle and right panels at the top). Thus, we manipulated the *visual perspective* of the body being watched (first person vs. third person) and the *timing* of the strokes applied (synchronous vs. asynchronous). In the 3PP Sync and 3PP Async conditions, the body of the mannequin was presented in the HMDs in a position that was rotated 180 degrees relative to

the participant's point of view, with its feet 0.5 meters away from the participant's feet (Figure S1b).

Experiment 3 consisted of two experimental designs (Figure S1c, far right panel). First, in a two-by-two factorial design, we varied the synchronicity of the visuotactile stimulation (synchronous or asynchronous) and the perceived integrity of the body and the right hand (attached or detached hand). Under these conditions, the participant viewed from the first-person visual perspective either the mannequin's intact body or the detached mannequin's right hand (without a body). The visuotactile stimulation was always applied to the right hand (Figure S1b, lower panels). The purpose of this factorial design was to identify areas that showed greater effect of synchrony when the hand was attached to a body than when it was perceived as an isolated detached limb (interaction term in the factorial design).

In the second design of experiment 3, we elicited the full body illusion by stimulating two different body parts of the intact mannequin (i.e., the abdomen and the hand). Thus, this design consisted of four conditions with synchronous or asynchronous visuotactile stimulation on the abdomen or the right hand. This design allowed us to look for areas showing increases in activity during the synchronous condition irrespectively of which body part was being stimulated, and this increased activity was tested in a conjunction analysis. Thus, in total, experiment 3 included six separate conditions split up into two designs that tested different hypotheses (Figure S1c, right panel, and Figure S1d, lower panel).

In all three studies, the experimenter stood on the right side of the participant and applied the touches with her index finger using small finger movements only, while standing as still as possible to minimize potential movement-induced distortions in the magnetic field. Each touch stimuli corresponded to a small five-centimeter-long brisk stroke. To achieve identical numbers of tactile stimuli under all conditions (n= 30 in each epoch; see below), the experimenter listened to audio commands delivered via the MRI-compatible headphones. The presentation of these auditory commands was digitally synchronized with the video sequences shown to the participants using Presentation (Presentation 13.1, build 05.30.09, Neurobehavioral Systems, Inc., www.neurobs.com). The same audio files were used when making the video recordings of the touches applied to the mannequin's body, ensuring perfect synchronization between the visual and tactile stimuli applied to the participant's abdomen during the scans in the two synchronous conditions. In the asynchronous conditions, the experimenter followed the same audio commands, but the video recordings were delayed by one second, introducing asynchrony between the seen and felt touches, which significantly diminishes the illusion [3]. During the scans, the experimenter was blind to the visual stimulus presented to the participants, eliminating any unintentional biases in the way the touches were applied under the different conditions. The participants were instructed to look at the location on the body being stimulated and to relax. The rationale for having passive subjects was to eliminate any potential fronto-parietal activation due to performing, or preparing, an active task.

Each condition epoch lasted 35 seconds. The conditions in experiments #1 and #2 were grouped in three blocks of four epochs, such that every condition was repeated three times within a scanning run. In the third experiment, the condition epochs were grouped in two blocks of six per scanning run (Supplementary Fig. S1d). Between each condition within a block, there was a short break lasting 3 seconds, during which the participants looked at a blank black screen and no touches were applied. After each block of four conditions (in experiments #1 and #2) or six conditions (in experiment 3), there was a 20-second baseline rest period, during which the participants were instructed to look at a black screen while no tactile stimuli were being

administered. In experiments #1 and #2, each run consisted of 171 volumes and lasted for 513 seconds, and the three runs comprising the experiment were performed successively, with a break of approximately three minutes between each run. In experiment 3, each run comprised 163 volumes and lasted 489 seconds, with a total of four runs with approximately three-minute-long breaks between runs.

Behavioral pilot experiments revealed that about 10 seconds of synchronous visuotactile stimulation is needed to elicit a vivid illusion of owning the mannequin's body (see Supplementary Results). Therefore, to ensure that the analysis used MRI image volumes sampled during intervals of sustained perceptual illusion, we excluded the first 10 seconds of each condition by modeling them as 'conditions of no interest' in the general linear model and modeled only the remaining 25 seconds periods as the experimental conditions (this procedure has been used before in fMRI experiments with the rubber-hand illusion [1, 42]).

Post-Scan Illusion Ratings and Calculation of Illusion Index

At the end of the scanning procedures in experiments # 1 and # 2, all subjects were requested to remain in the scanner for an additional 5 minutes, during which they were presented with each of the four conditions again. At the end of each condition, four written statements were presented on the HMDs: two statements were designed to capture the experience of the illusion (S1: "I felt as if I was watching my own body being touched" and S2: "I felt as if the hand I saw was the one touching me"), whereas the other two statements served as controls (S3: "I felt as if I had two bodies" and S4: "I felt as if my body had turned into plastic"; the word 'plastic' was replaced with the word 'wood' in the conditions where a wooden block was presented). The participants were asked to report the degree of their agreement with each statement verbally, using a rating scale from 0 to 100 percent. These values were then used to calculate an illusion index, to quantify the subjectively experienced strength of the illusion for each participant. For both fMRI experiments, the respective indices were calculated using the following formulas:

fMRI #1: [(S1_Body_Sync – S1_Body_Async) + (S2_Body_Sync – S2_Body_Async)] – (S1_Wood_Sync – S1_Wood_Async) + (S2_Wood_Sync – S2_Wood_Async)]/2.

fMRI #2: [(S1_1PP_Sync – S1_1PP_Async) + (S2_1PP_Sync – S2_1PP_Async)] – (S1_3PP_Sync – S1_3PP_Async) + (S2_3PP_Sync – S2_3PP_Async)]/2.

Thus, an index greater than 0 would indicate that the participant experienced a greater illusion in the Body Sync or 1PP Sync conditions, in comparison to the three controls; on the other hand, a score ≤ 0 would mean that the participant did not experience the illusion.

Acquisition and Analysis of Functional Imaging Data

We used functional magnetic resonance imaging (fMRI) at 3T (TIM Trio, Siemens, Erlangen, Germany) to measure BOLD-signal changes in cortical activity with a T2*-sensitive echo planar imaging pulse sequence (repetition time 3000 ms; echo time 40 ms; flip angle 90°; 47 near-axial slices; 3-mm isotropic voxel size; matrix size 58 by 76). Images were acquired using a 12-channel phased-array head coil. A high-resolution T1-weighted structural scan at 1-mm isotropic voxel size was also acquired for each subject for anatomical registration, segmentation and display. To minimize head motion, we stabilized the subject's head with the help of foam padding.

Statistical Parametric Mapping

The fMRI data were analyzed with 'Statistical Parametric Mapping Software 8' (SPM8; http//:www.fil.ion.ucl.ac.uk/spm; Wellcome Department of Cognitive Neurology, London). The functional images were motion-corrected, co-registered with the high-resolution structural scan, normalized to the MNI reference space and smoothed with an 8-mm FWHM Gaussian kernel. For each of the experimental conditions described above, we defined two regressors, modeling the first 10 and the subsequent 25 seconds of each stimulation period, respectively (see above). The realignment parameters were included in the model as regressors of no interest, to account for residual head motion. Each condition was modeled as a boxcar function and convoluted with the standard SPM8 hemodynamic response function.

To accommodate inter-subject variability, the contrast images from all subjects were entered into a random effect group analysis (second-level analysis). In the factorial design, we only reported peaks of activation surviving the statistical threshold of $p < 0.05$, corrected for multiple comparisons. For areas where we had *a priori* hypotheses, we used the significance level that corresponded to $p < 0.05$ corrected for multiple comparisons using a small volume correction (see Table S1). In the rest of the brain, where we did not have such *a priori* hypotheses, we used the topological peak-FDR as implemented in SPM8. In a purely descriptive approach, we also list in the tables all activation peaks that survive $p < 0.001$ (uncorrected), to illustrate the specificity of the significant activations; for the same reason, in the figures, the activation maps had a significance threshold of $p < 0.001$ (uncorrected), meaning that some non-specific activations can also be seen in these displays. Importantly, the significant peaks of activations ($p < 0.05$, corrected) upon which we based our conclusions are clearly marked in the figures with blue crosses or white circles.

We defined several linear contrasts in the general linear model to test our hypotheses. First, we analyzed the interaction terms in the factorial designs using the following contrasts: (Body Sync – Body Async) – (Wood Synch – Wood Async) in the first study; (1PP Sync – 1PP Async) – (3PP Synch – 3PP Async) in the second study; (Attached Hand Sync– Attached Hand Async) – (Detached Hand Sync – Detached Hand Async) in the third experiment. In the second experiment, we also defined an interaction contrast to search for areas showing the greatest activity when the mannequin was observed from the third-person perspective, while perceiving synchronized visuotactile stimulation, using the formula: (3PP Sync – 3PP Asynch) – (1PP Sync – 1PP Async).

In study 3, we looked for areas showing increases in activity during the full-body illusion regardless of which of the two body parts was being stimulated (hand or abdomen). First, we analyzed each of the two body-part-specific contrasts individually (Abdomen Sync – Abdomen Async) and (Attached Hand Sync – Attached Hand Async), respectively and displayed the results on a single brain (see Figure 4b). To formally test for clusters of active voxels that were commonly activated by the hand and abdominal stimulation, we employed the following conjunction analysis: (Abdomen Sync – Abdomen Async) $\cap$ (Attached Hand Sync – Attached Hand Async). We also identified body-part-specific regions that were only activated when a particular body part was stimulated. To identify abdomen-specific regions, we used the contrast (Abdomen Sync – Abdomen Async) with the exclusive mask (Attached Hand Sync – Attached Hand Async; $p < 0.001$, uncorrected) (the red clusters in Figure 4b). By using an exclusive masking procedure we ensured that voxels classified as abdomen-specific were not activated by the hand stimulation. In the same way, we defined the hand-specific regions using the contrast (i.e., Attached Hand Sync – Attached Hand Async), with (Abdomen Sync – Abdomen Async)

serving as an exclusive mask (the yellow clusters in Figure 4b). In study 3, we also performed a post-hoc analysis in which we investigated whether there were modulations in the BOLD-signal in the abdomen-specific region (at the peaks) when the hand was stimulated [(Attached Hand Sync– Attached Hand Async) – (Detached Hand Sync – Detached Hand Async)]. This procedure is valid, as the data used to define the abdomen-specific peaks were independent from the data used to define the interaction term in the factorial design with the four hand-stimulation conditions.

In experiments #1 and #2, we used a second-level regression model (as implemented in SPM8) to identify the brain regions in which the activity was related to the strength of the illusion as rated by the participants after the scans (using the illusion index described above). We defined a covariate corresponding to the illusion index for each participant and used the contrast images from the interaction term to search for areas in the whole brain showing a systematic relationship between illusion strength and the BOLD response (Figure 3).

Multivoxel Pattern Analysis

To examine the encoding of generalized full-body ownership in detail, we used multivoxel pattern analysis (MVPA) on the data from experiment 3. The functional images were pre-processed using SPM 8 in the same way as in the traditional univariate analyses described above (i.e., motion corrected, co-registered with the high-resolution structural scan, normalized to the MNI reference space and smoothed with an 8-mm FWHM Gaussian kernel). Subsequent MVPA-specific pre-processing was performed with the Princeton Multi-Voxel Pattern Analysis Toolbox (www.pni.princeton.edu/mvpa). Each voxel's response was normalized relative to the average of the time-course within each scan. The first 10 seconds of each condition epoch were discarded (as in the SPM analyses described above), and single trial estimates were formed by averaging across the subsequent 25 seconds of each epoch. Given the relatively long duration of the epochs and that the first 10 seconds were discarded, no explicit modeling of the hemodynamic response function was required.

Following up on the results from the SPM conjunction analysis (see above), we focused the MVPA on the left ventral premotor cortex. This region of the brain was delineated in an unbiased fashion using the WFU PickAtlas toolbox for SPM (www.wfubmc.edu). Specifically, we selected the precentral gyrus and set the z axis value to 45 to limit the region to the ventral portion of the premotor cortex (PMv).

We searched this PMv region of interest for voxels carrying illusion-related information using locally-multivariate Monte Carlo brain mapping [43]. Similar to the Searchlight algorithm [44], the Monte Carlo mapping approach evaluates multivariate information in search volumes of pre-defined size and shape. Instead of sequentially centering the search volume on each voxel in the brain, the Monte Carlo approach utilizes random sampling and information-averaging for substantially improved efficiency (but with no loss in sensitivity) [43]. A linear support vector machine (in the LIBSVM implementation; http://www.csie.ntu.edu.tw/wcjlin/libsvm/, with fixed regularization parameter C = 1) was used to model the conditions, and the proportion of correctly decoded trials (in an independent test dataset; see below) was used to indicate the multivariate information content. The search volume size was set to 4 mm.

We performed several analyses to examine the mechanisms underlying generalized whole-body ownership. First, we applied the Monte Carlo algorithm to search the PMv for voxels representing body-part-independent ownership, i.e., where the SVMs could generalize from one body part to another. To this end, the SVMs were trained to decode Abdomen Sync from

Abdomen Async (9 epochs of each category, 18 epochs in total) and were tested on attached Hand Sync vs. attached Hand Async (also 9 epochs of each category, 18 epochs in total). This approach specifically targets the illusory effects (i.e., contrasting synchronous versus asynchronous stimuli) while directly reflecting any generalization in multivoxel response pattern of the illusion induced by the different body parts; only groups of voxels reflecting robustly similar neural representations of the illusion will obtain high decoding scores. The procedure was repeated independently in each subject to produce multivariate maps reflecting voxel-wise generalization accuracies across body parts.

Nonparametric permutation testing was used to assess the significance of the generalization accuracies of each voxel in the individual maps [45]. To this end, the identical Monte Carlo mapping procedure above was iterated 999 times with different data label permutations. Voxel-wise p-values were computed as the proportion of permuted values that were at least as large as the true generalization accuracy obtained for that voxel. This procedure allowed thresholding of the maps to only indicate voxels that reached significant generalization accuracy. All subsequent analysis was restricted to these voxels.

We then isolated voxels that demonstrated significant generalization across body parts ($p < 0.05$, permutation test with 999 iterations). We used a lenient threshold and no adjustment for multiple comparisons to identify an inclusive group of 'generalization voxels' for subsequent control analyses.

First, we ran a control analysis to verify the reverse generalization, i.e., that the illusion induced on the hand could also generalize to the abdomen. To this end, the SVMs were trained to decode attached Hand Sync from attached Hand Async and were tested on Abdomen Sync vs. Abdomen Async. Second, we ran a control analysis to rule out the possibility that the generalization voxels reflected multivoxel information related to unspecific effects of synchronous visual and tactile stimulation. We reasoned as follows: if the classifiers were detecting visuotactile synchrony rather than a whole-body ownership effect, they should also generalize to the context in which the hand is perceived as a detached limb. We therefore applied the Monte Carlo algorithm using exactly the same settings as before but this time within the generalization voxels and in search of voxels where SVMs trained to decode Abdomen Sync from Abdomen Async (as above) could also decode detached Hand Sync from detached Hand Async. Using the same logic, we also tested for voxels where SVMs trained to decode attached Hand Sync from attached Hand Async could generalize to decode detached Hand Sync from detached Hand Async. As stated previously, we predicted that the classifiers would fail to generalize in the context of the detached hand, indicating that the classifiers in our first analysis detected multivoxel information specifically related to full-body ownership.

Lastly, we tested for body-part-specific effects within the generalization voxels by searching for voxels where SVMs could decode attached Hand Sync from Abdomen Sync. In contrast to the previous analyses where we used matched pairs of conditions to train and test the classifiers, a cross-validation scheme for training and testing was required here. A robust hold-out validation approach was therefore employed, where approximately 60% of the stimuli (i.e., 10 trials, with a balanced number from each condition) were used to train the classifier, and the remaining 40% (8 trials) were used to validate the SVM model. This was repeated twice for each search volume, and the average was taken as a measure of the decoding performance.

To compare the decoding performances across the conditions, a group decoding performance measure was formed by taking the average across the peak decoding accuracies of each subject (Figure 4c). We tested the significance level of this group average by applying the

identical procedure to all 999 permuted maps (i.e., in each permuted map we averaged across the peak individual decoding accuracies). The p-value of the group average was computed as the proportion of permuted values that were at least as large as the true value.

Supplemental References

1. Ehrsson, H.H., Spence, C., and Passingham, R.E. (2004). That's My Hand! Activity in Premotor Cortex Reflects Feeling of Ownership of a Limb. Science *305*, 875-877.
2. Ehrsson, H.H., Fagergren, A., Jonsson, T., Westling, G., Johansson, R.S., and Forssberg, H. (2000). Cortical activity in precision- versus power-grip tasks: an fMRI study. J Neurophysiol *83*, 528-536.
3. Petkova, V.I., and Ehrsson, H.H. (2008). If I Were You: Perceptual Illusion of Body Swapping. PloS One *3*, e3832.
4. Fogassi, L., Gallese, V., di Pellegrino, G., Fadiga, L., Gentilucci, M., Luppino, G., Matelli, M., Pedotti, A., and Rizzolatti, G. (1992). Space coding by premotor cortex. Exp. Brain Res. *89*, 686-690.
5. Graziano, M., and Gross, C.G. (1998). Spatial maps for the control of movement. Curr. Opin. Neurobiol. *8*, 195-201
6. Graziano, M., and Botvinick, M. (2002). How the brain represents the body: insights from neurophysiology and psychology. In Common Mechanisms in Perception and Action: Attention and Performance XIX., W. Prinz and B. Hommel, eds. (Oxford: Oxford University Press), pp. 136-157.
7. Rizzolatti, G., Luppino, G., and Matelli, M. (1998). The organization of the cortical motor system: new concepts. Electroencephalogr Clin. Neurophysiol. *106*, 283-296.
8. Fogassi, L., Gallese, V., Fadiga, L., Luppino, G., Matelli, M., and Rizzolatti, G. (1996). Coding of peripersonal space in inferior premotor cortex (area F4). J Neurophysiol. *76*, 141-157.
9. Graziano, M. (1999). Where is my arm? The relative role of vision and proprioception in the neuronal representation of limb position. Proc. Natl. Acad. Sci. USA *96*, 10418-10421.
10. Graziano, M., Hu, X.T., and Gross, C.G. (1997). Visuospatial Properties of Ventral Premotor Cortex. J. Neurophysiol. *77*, 2268-2292.
11. Avillac, M., Ben Hamed, S., and Duhamel, J.-R. (2007). Multisensory Integration in the Ventral Intraparietal Area of the Macaque Monkey. J. Neurosci. *27*, 1922-1932.
12. Avillac, M., Deneve, S., Olivier, E., Pouget, A., and Duhamel, J.-R. (2005). Reference frames for representing visual and tactile locations in parietal cortex. Nat. Neurosci. *8*, 941-949.
13. Colby, C.L., Duhamel, J.R., and Goldberg, M.E. (1993). Ventral intraparietal area of the macaque: anatomic location and visual response properties. J Neurophysiol. *69*, 902-914.
14. Duhamel, J.-R., Colby, C.L., and Goldberg, M.E. (1998). Ventral Intraparietal Area of the Macaque: Congruent Visual and Somatic Response Properties. J. Neurophysiol. *79*, 126-136.

15. Graziano, M., Cooke, D.F., and Taylor, C.S.R. (2000). Coding the Location of the Arm by Sight. Science *290*, 1782-1786.
16. Iriki, A., Tanaka, M., and Iwamura, Y. (1996). Coding of modified body schema during tool use by macaque postcentral neurones. Neuroreport *7*, 2325-30
17. Graziano, M., and Gross, C.G. (1993). A bimodal map of space: somatosensory receptive fields in the macaque putamen with corresponding visual receptive fields. Exp. Brain Res. *97*, 96-109.
18. Graziano, M., and Gandhi, S. (2000). Location of the polysensory zone in the precentral gyrus of anesthetized monkeys. Exp. Brain Res. *135*, 259-266.
19. Gentilucci, M., Scandolara, C., Pigarev, I., and Rizzolatti, G. (1983). Visual responses in the postarcuate cortex (area 6) of the monkey that are independent of eye position. Exp. Brain Res. *50*, 464-468.
20. Ishida, H., Nakajima, K., Inase, M., and Murata, A. (2010). Shared Mapping of Own and Others' Bodies in Visuotactile Bimodal Area of Monkey Parietal Cortex. J. Cogn. Neurosci. *22*, 83-96.
21. Bremmer, F., Schlack, A., Duhamel, J.-R., Graf, W., and Fink, G.R. (2001). Space Coding in Primate Posterior Parietal Cortex. NeuroImage *14*, S46-S51.
22. Driver, J., and Noesselt, T. (2008). Multisensory Interplay Reveals Crossmodal Influences on 'Sensory-Specific' Brain Regions, Neural Responses, and Judgments. Neuron *57*, 11-23.
23. Macaluso, E., and Driver, J. (2005). Multisensory spatial interactions: a window onto functional integration in the human brain. Trends in Neurosciences *28*, 264-271.
24. Gentile, G., Petkova, V.I., and Ehrsson, H.H. (2011). Integration of Visual and Tactile Signals From the Hand in the Human Brain: An fMRI Study. J. Neurophysiol. *105*, 910-922.
25. Lloyd, D.M., Shore, D.I., Spence, C., and Calvert, G.A. (2003). Multisensory representation of limb position in human premotor cortex. Nat. Neurosci. *6*, 17-18.
26. Brozzoli, C., Gentile, G., Petkova, V.I., and Ehrsson, H.H. (2011). fMRI-adaptation reveals a cortical mechanism for the coding of space near the hand. J. Neurosci. In press
27. Makin, T.R., Holmes, N.P., and Zohary, E. (2007). Is That Near My Hand? Multisensory Representation of Peripersonal Space in Human Intraparietal Sulcus. J. Neurosci. *27*, 731-740.
28. Luppino, G., Murata, A., Govoni, P., and Matelli, M. (1999). Largely segregated parietofrontal connections linking rostral intraparietal cortex (areas AIP and VIP) and the ventral premotor cortex (areas F5 and F4). Exp. Brain Res. *128*, 181-187.
29. Matelli, M., Camarda, R., Glickstein, M., and Rizzolatti, G. (1986). Afferent and efferent projections of the inferior area 6 in the macaque monkey. J. Comp. Neurol. *251*, 281-298.
30. Muakkassa, K.F., and Strick, P.L. (1979). Frontal lobe inputs to primate motor cortex: evidence for four somatotopically organized 'premotor' areas. Brain Res. *177*, 176-182.
31. Graziano, M., and Cooke, D. (2006). Parieto-frontal interactions, personal space, and defensive behavior. Neuropsychologia *44*, 845-859.
32. Stein, B.E. (1998). Neural mechanisms for synthesizing sensory information and producing adaptive behaviors. Exp. Brain Res. *123*, 124-135.

33. Stein, B.E., and Stanford, T.R. (2008). Multisensory integration: current issues from the perspective of the single neuron. Nat. Rev. Neurosci. *9*, 255-266.
34. Corbetta, M., and Shulman, G.L. (2002). Control of goal-directed and stimulus-driven attention in the brain. Nat. Rev. Neurosci. *3*, 201-215.
35. Downar, J., Crawley, A.P., Mikulis, D.J., and Davis, K.D. (2000). A multimodal cortical network for the detection of changes in the sensory environment. Nat. Neurosci. *3*, 277-283.
36. Blanke, O., Landis, T., Spinelli, L., and Seeck, M. (2004). Out-of-body experience and autoscopy of neurological origin. Brain *127*, 243-258.
37. Lenggenhager, B., Smith, S., and Blanke, O. (2006). Functional and neural mechanisms of embodiment: importance of the vestibular system and the temporal parietal junction. Rev. Neurosci. *17*, 643-657.
38. James, W. ed. (1890). Prinicples of Psychology (New York: H Holt and Company).
39. Huk, A.C., Ress, D., and Heeger, D.J. (2001). Neuronal Basis of the Motion Aftereffect Reconsidered. Neuron *32*, 161-172.
40. Ehrsson, H.H., Kito, T., Sadato, N., Passingham, R.E., and Naito, E. (2005). Neural Substrate of Body Size: Illusory Feeling of Shrinking of the Waist. PLoS Biol *3*, e412.
41. Naito, E., Roland, P.E., and Ehrsson, H.H. (2002). I Feel My Hand Moving: A New Role of the Primary Motor Cortex in Somatic Perception of Limb Movement. Neuron *36*, 979-988.
42. Ehrsson, H.H., Holmes, N.P., and Passingham, R.E. (2005). Touching a Rubber Hand: Feeling of Body Ownership Is Associated with Activity in Multisensory Brain Areas. J. Neurosci. *25*, 10564-10573.
43. Björnsdotter, M., Rylander, K., and Wessberg, J. (2011). A Monte Carlo method for locally multivariate brain mapping. NeuroImage *56*,508-16.
44. Kriegeskorte, N., Goebel, R., and Bandettini, P. (2006). Information-based functional brain mapping. Proc. Natl. Acad. Sci. USA *103*, 3863-3868.
45. Nichols, T.E., and Holmes, A.P. (2002). Nonparametric permutation tests for functional neuroimaging: A primer with examples. Hum. Brain Mapp. *15*, 1-25.